Colloid Polym Sci (2009) 287:323–334
DOI 10.1007/s00396-008-1969-9

ORIGINAL CONTRIBUTION

# Swelling–shrinking behaviors of poly(*N*-isopropylacrylamide) and poly(*N*-*n*-propylacrylamide) gels prepared by chemical and radiation crosslinking methods

**Masami Takekawa · Etsuo Kokufuta**

Received: 8 October 2008 / Revised: 13 November 2008 / Accepted: 15 November 2008 / Published online: 6 December 2008


**Abstract** The swelling and shrinking kinetics of thermosensitive gels based on *N*-isopropylacrylamide (NiPAAm) and *N*-*n*-propylacrylamide (NnPAAm) were studied. Four gels cylindrical in shape were prepared by two different methods: $\gamma$-ray irradiation to aqueous solutions of poly(NiPAAm) (PNiPAAm) or poly(NnPAAm) (PNnPAAm) and redox polymerization of NiPAAm or NnPAAm monomer using *N*,*N*′-methylenebisacrylamide as a crosslinker. There were a few differences in the swelling kinetics among these gels. However, a marked difference was observed in the shrinking processes, the rate of which was faster in the order of radiation-crosslinked PNiPAAm gel > radiation-crosslinked PNnPAAm gel > chemically crosslinked PNnPAAm gel > chemically crosslinked PNiPAAm gel. This difference was discussed in terms of the microscopic structure of the gels, which was studied by light scattering techniques. It was found that the static inhomogeneities frozen in the chemically and radiation-crosslinked gels play a key role in their shrinking kinetics.

**Keywords** *N*-Isopropyl- and *N*-*n*-propylacrylamide gels · *N, N*′-Methylenebisacrylamide and $\gamma$-ray crosslinking · Swelling–shrinking kinetics · Light scattering · Structural inhomogeneity

M. Takekawa
Graduate School of Life and Environmental Sciences,
University of Tsukuba,
Tsukuba, Ibaraki 305-8572, Japan

E. Kokufuta (✉)
Graduate School of Life and Environmental Sciences and Institute of Applied Biochemistry, University of Tsukuba,
Tsukuba, Ibaraki 305-8572, Japan
e-mail: kokufuta@sakura.cc.tsukuba.ac.jp

## Introduction

Many sorts of polymer gels undergo abrupt and reversible changes in volume in response to external stimuli such as temperature, pH, or the nature of the solvent. This phenomenon known as the volume phase transition in gels [1, 2] has received continuous attention over the past 30 years in both fundamental and applied research. Among these, the kinetics of swelling and shrinking of gels is one of the most important subjects.

Tanaka and his coworkers [3–5] have studied a theory of the swelling–shrinking kinetics of gels and compared it with their experiment results. Then, the characteristic time ($\tau$) taken for a gel to swell or shrink was given by

$$\tau \propto \frac{l^2}{D} \tag{1}$$

where $l$ denotes the characteristic linear dimension of the gel and $D$ is the collective diffusion coefficient of the networks. This equation means that the time for a gel to swell or shrink depends on its size, e.g., the radius of a spherical gel. Thus, the gels seem to undergo a fast volume change as the term of $l$ is reduced. A candidate falling into this criteria would be gel particles with diameters in the range of several tens to several hundreds of nanometers, often referring to as “microgels” or “nanogels.” However, the swelling–shrinking kinetics of such gel particles has not yet been studied in detail through the direct measurement of particle sizes as a function of time, probably because of the lack of experimental techniques. Indeed, the fast kinetics of microgels has been predicted from the studies of (1) the diffusion rate of solutes into or out of the gel particles (e.g., see [6]) and (2) the permeation rate of solvents through the pore formed among the gel particles (e.g., see [7]). In both examples [6, 7], the temperature responsible microgels of

*N*-isopropylacrylamide (NiPAAm) were employed; thus, the measurements were performed below and above a lower critical solution temperature (LCST) of poly(NiPAAm) (PNiPAAm).

Another candidate seems to be macroporous gels having a large pore size, a high pore volume, and a high specific surface area, a good example of which is the opaque gels of PNiPAAm obtained at temperatures above the LCST [8–11]. The observed rapid volume change of such macroporous gels was then interpreted by assuming that their bodies are made up of minute domains of densely and sparsely crosslinked gel networks; therefore, the $l$ in Eq. 1 should be reduced.

A technique for achieving a fast deswelling kinetics of NiPAAm gels without relying on reduction of $l$ in Eq. 1 has been reported [12]. This was based on the use of a macromonomer which is composed of the NiPAAm main chains and has a vinyl group at the one end; thus, the crosslinking with *N*,*N*′-methylenebisacrylamide (Bis) yields a gel network to which many graft chains are bound, i.e., a comb-type grafted NiPAAm gel. The gel obtained was transparent in appearance, like conventional Bis-crosslinked NiPAAm gels, but exhibited a very rapid rate of shrinking in response to a change in temperature of 10 °C to 40 °C. Since the shrinking rate was found to vary depending on the length of graft chains, it was concluded that the thermal collapse of graft chains "bound to the network" plays a key role in an overall gel collapse. This should be distinct from the dynamic property of conventional gels which is dominated by the diffusion-limited transport of polymeric components of the network in a solvent as characterized by the term $D$ in Eq. 1.

The swelling–shrinking kinetics of NiPAAm gels has also been studied from a totally different point of view from the concept in Eq. 1 [13]. Then, two types of the gels were employed; one is obtained from the chemical crosslinking of NiPAAm (monomer) with Bis and the other is from the radiation crosslinking with $\gamma$-rays of an aqueous "raw" PNiPAAm solution (i.e., reaction mixture after polymerizing the monomer solution which is the same as used in the chemical crosslinking, but free from the crosslinker). It was reported that a rapid shrinking takes place when the gels were prepared at low levels of crosslinker (Bis or irradiation dose) and/or at high temperatures (27 °C and 30 °C), regardless of the preparation method. Also reported was the observation of structural differences between the gel networks formed by the chemical and the radiation crosslinking, although this microscopic feature was little discussed in connection with the macroscopically observed swelling–shrinking kinetics.

As seen from the above [1] to [13], a question has still remained about a correlation of the swelling–shrinking kinetics of gels with their microscopic structures, on which we focused our attention. Before describing the purpose of the present work, we briefly introduce the structural inhomogeneity of the gel network, based on the article of Sato-Matsuo et al. [14]. They examined Bis-crosslinked NiPAAm gels using a microscope laser light scattering technique and observed a fluctuating speckle pattern due to highly nonuniform spatial distributions of polymer network concentration and crosslinking density in the gel. These inhomogeneities were then considered to have two origins: One is the dynamic critical fluctuations of the polymer solution at the onset of gelation, and the other is the domain formation due to the microphase separation, both of which are directly related to the phase equilibrium properties of the gel during the gelation process. Such fluctuations of polymer density are permanently frozen in the gel structure. In addition to these permanent spatial fluctuations, a polymer network undergoes thermal dynamic concentration fluctuations. These three types of fluctuations, two static and one dynamic, account for the nature of gel inhomogeneities.

The conventional technique of dynamic light scattering (DLS) can now be used to study the structural inhomogeneity of gels (e.g., see [13] and references therein). The DLS data may be analyzed by the partial heterodyne method proposed by Joosten et al. [15], in which an intensity–intensity time correlation function ($g^{(2)}(\tau)$) obtained by DLS for a position of a gel sample is given as:

$$g^{(2)}(\tau) = \beta\sigma_{\mathrm{I}}^2 \exp\left[-2D_{\mathrm{A}}q^2\tau\right] + 1 = \sigma_{\mathrm{I,obs}}^2 \exp\left[-2D_{\mathrm{A}}q^2\tau\right] + 1 \quad (2)$$

Here, $\beta$ ($\equiv \sigma_{\mathrm{I,obs}}^2 \big/ \sigma_{\mathrm{I}}^2$) denotes the instrumental coherence factor ranging from larger than zero to smaller than unity, $\sigma_{\mathrm{I}}^2$ is the initial amplitude of $g^{(2)}(\tau)$, and $\sigma_{\mathrm{I,obs}}^2$ is that at observation. Moreover, $D_{\mathrm{A}}$ is the apparent diffusion coefficient, $q$ is the magnitude of the scattering vector, and $\tau$ is the time difference between the photons and must be distinguished from the $\tau$ in Eq. 1. As a result, from the DLS for a given point (or position) of a gel, we may estimate the $D_{\mathrm{A}}$ and also the time-averaged scattering intensity ($\langle I\rangle_{\mathrm{T}}$). By repeating the measurements (e.g., 100 times) at different positions for the same gel sample, various sets of the $D_{\mathrm{A}}$ and $\langle I\rangle_{\mathrm{T}}$ data can be obtained. Using these data, the dynamic component of the concentration fluctuations ($\langle I_{\mathrm{F}}\rangle_{\mathrm{T}}$) may be evaluated from

$$D_{\mathrm{L}} = \frac{D_{\mathrm{A}}}{2 - \langle I_{\mathrm{F}}\rangle_{\mathrm{T}} / \langle I\rangle_{\mathrm{T}}} \quad (3)$$

where $D_{\mathrm{L}}$ is a diffusion coefficient often referring to as "cooperative" or "collective" diffusion coefficient. It is still not clear whether the $D_{\mathrm{L}}$ is equivalent to the $D$ in Eq. 1 but evident that $D_{\mathrm{A}}=D_{\mathrm{L}}$ in a homodyne mode and $D_{\mathrm{A}}=2D_{\mathrm{L}}$ in a heterodyne mode. Another important information from the

DLS of gels is the observation of fluctuating speckles, from which we can obtain the ensemble-averaged scattering intensity ($\langle I\rangle_E$) as the average of $\langle I\rangle_T$. Since the $\langle I\rangle_E$ is found to be an indication of the static inhomogeneity of gel networks, we may examine the microscopic feature of gels.

Taking the above into account, we attempted to study the swelling–shrinking kinetics of gels, together with their microscopic characteristics. The four gel samples were prepared by the chemical and radiation crosslinking methods using the monomer as well as the polymer of NiPAAm or *N*-*n*-propylacrylamide (NnPAAm), i.e., gels from NiPAAm (monomer) crosslinked with Bis and from PNiPAAm (polymer) crosslinked by γ-ray irradiation, as well as from NnPAAm (monomer) crosslinked with Bis and from poly(NnPAAm) (PNnPAAm) crosslinked by γ-ray irradiation. Abbreviation of these gel samples was shown in Table 1. It has been known that RPNG (i.e., radiation-crosslinked PNnPAAm gel) undergoes a volume phase transition at a temperature lower by about 10 °C than CIG (chemically crosslinked NiPAAm gel; e.g., see [16]). Thus, the use of both NiPAAm and NnPAAm-based gels would facilitate the discussion on how the inhomogeneity of gels affects their swelling–shrinking kinetics.

## Experimental

*Materials* The NiPAAm monomer (kindly supplied by Kojin Chemical Co., Tokyo, Japan) was recrystallized in *n*-hexane to remove a polymerization inhibitor (*p*-methoxyphenol). The NnPAAm monomer was synthesized and purified according to the same method as used in [16]. Ammonium persulfate (APS), *N*,*N*,*N*′,*N*′-tetramethylethylenediamine (TEMED) and Bis were commercially obtained from Wako Pure Chemical Co. (Tokyo, Japan) and used as received. The polymers (PNiPAAm and PNnPAAm) were synthesized by radical polymerization using benzene as the solvent and α,α′-azobis(isobutyronitrile) as the initiator [16, 17]. The polymerization was carried at 60 °C for 30 min under nitrogen. The resulting reaction mixture was slowly poured into *n*-hexane to precipitate the polymer, which was then separated by filtration, washed with *n*-hexane, and dried in a vacuum. Further purification was carried out by dialyzing an aqueous polymer solution against distilled water for a week. We then employed a cellulose ester dialysis membrane (Spectra/Por® CE) having a molecular weight cutoff of 100,000. The dialyzed solution was lyophilized and finally dried under reduced pressure at 50 °C for 3 days. We determined the weight-average molecular weight ($\overline{M}_w$) by both static light scattering (SLS) and gel permeation chromatography (GPC) as well as the number-average molecular weight ($\overline{M}_n$) by GPC; for PNiPAAm, $\overline{M}_w = 5.53\times10^5$ (SLS) and $5.40\times10^5$ (GPC) and $\overline{M}_n = 3.45\times10^5$ (GPC); and for PNnPAAm, $\overline{M}_w = 3.61\times10^5$ (SLS) and $3.56\times10^5$ (GPC) and $\overline{M}_n = 1.98\times10^5$ (GPC). The $\overline{M}_w/\overline{M}_n$ was within 1.6–1.8, indicating that both polymers have a narrow molecular weight distribution.

**Table 1** Abbreviations for the gels used in this study

| Abbreviation | Source | Crosslinking |
|---|---|---|
| CIG | NiPAAm (monomer) | Chemical with Bis |
| CNG | NnPAAm (monomer) | Chemical with Bis |
| RPIG | PNiPAAm (polymer) | Radiation with γ-ray |
| RPNG | PNnPAAm (polymer) | Radiation with γ-ray |

*C* "chemically" crosslinked with Bis, *R* "radiation" crosslinked with γ-rays, *P* polymer, *I N-iso*propylacrylamide, *N N-n*-propylacrylamide, *G* gel

*Preparation of gels* The radiation-crosslinked gels (RPIG and RPNG) were prepared via the γ-ray irradiation of an aqueous oxygen-free solution of PNiPAAm or PNnPAAm. The polymer concentration was usually fixed at 5% (*w*/*w*) but varied from 1% to 10% (*w*/*w*) when a sol–gel phase diagram was studied as a function of irradiation dose. The dust-free polymer solution was transferred into a test tube (total volume ~5 ml; inner diameter ~9 mm), degassed well under a vacuum, and finally the tube was sealed. In the case of the preparation of small cylindrical gels for the swelling and shrinking measurements, glass capillaries with different inner diameters ($d_0$=0.29 to 3.4 mm) had previously been inserted in the test tube. The gelation was carried out in an ice bath at a dose rate of 1.56 kGy/h as a function of time, using γ-rays from a $^{60}$Co source.

The Bis-crosslinked gels (CIG and CNG) were prepared using an aqueous, dust, and oxygen-free monomer solution (i.e., pregel) containing either NiPAAm or NnPAAm and both Bis and TEMED (accelerator). The gelation was performed at ice-bath temperature under an $N_2$ atmosphere after uniform mixing of an APS solution (1 ml) with the pregel (9 ml) using a vortex mixer. The final concentrations of the chemicals were 49.8 mg/ml (440 mM) for NiPAAm or NnPAAm, 0.834 mg/ml (5.41 mM) for Bis, 0.4 mg/ml (1.75 mM) for APS, and 4.8 μl/ml (3.78 mg/ml ≈32.6 mM) for TEMED. The concentration of NiPAAm or NnPAAm plus Bis is equivalent to 5% *w*/*w* within experimental errors. For preparing the CIG and CNG samples with different crosslink densities, we changed the molar ratio of Bis to NiPAAm or NnPAAm so as to keep the concentration at 5% *w*/*w* under the fixed concentration of APS and TEMED. The other procedures were the same as those in the radiation crosslinking.

After the gelation was completed, the gel sample was taken out of the test tube. In the case of a fine cylindrical gel for the swelling measurements, we pulled it out of the

capillary. After thorough washing with distilled water, the sample for DLS was carefully collapsed with a hot water, inserted into a measuring cell (i.e., test tube having the same size as in the gelation) filled with distilled water, and then slowly swollen in the cell by cooling. The sample for the swelling measurements was cut into small pieces with an appropriate length to be used.

*Measurements of gel diameter* A section of the cylindrical gel was inserted into a water-jacketed microcell together with distilled water. The gel was then observed using a microscope with a calibrated scale, from which the images were recorded digitally on videotape as a function of time. The temperature was controlled within a range of ±0.05 °C with water circulating around the measuring cell. To determine the swelling and deswelling rates, the temperature surrounding the gel was changed very rapidly (within 15 s) using two water-circulating systems at desired temperatures. The size (i.e., diameter) of gel at a time was determined by a careful VTR image analysis.

*DLS experiments* The measurements were performed at fixed temperature (20±0.1 °C) and scattering angle (90°), using a dynamic light scattering spectrophotometer (DLS-7000, Otsuka Electronics Co., Japan). A 10-mW He–Ne laser with the wavelength of 632.8 nm was used as the incident beam. Time averaged intensity and the corresponding intensity-correlation function were determined with acquisition time of 1 min for each run. Both data were collected from 100 positions within the same gel by turning the cell tube at 18° around the vertical axis, the operation of which was repeated five times by a vertical difference of 3 mm.

## Results and discussion

### Sol–gel phase diagram

The phase diagram was studied to determine conditions of γ-ray irradiation for the preparation of RPIG and RPNG in Table 1. The gelation was then determined by a falling-ball method [18], in which we looked upon as a gel formed when a stainless steel ball did not fall for 5 min. A typical sol–gel phase diagram for PNiPAAm is shown in Fig. 1. It is found that the gelation occurs above a certain threshold of polymer concentration ($C_p$) and of irradiation dose ($D_{ir}$), often referring to as the critical polymer concentration ($C_{pc}$) and the gelation dose ($D_g$), respectively. A very similar result was obtained in the case of PNnPAAm. Both results also agreed with the general trend in the formation of hydrogels with γ-rays, for example, the gelation of aqueous

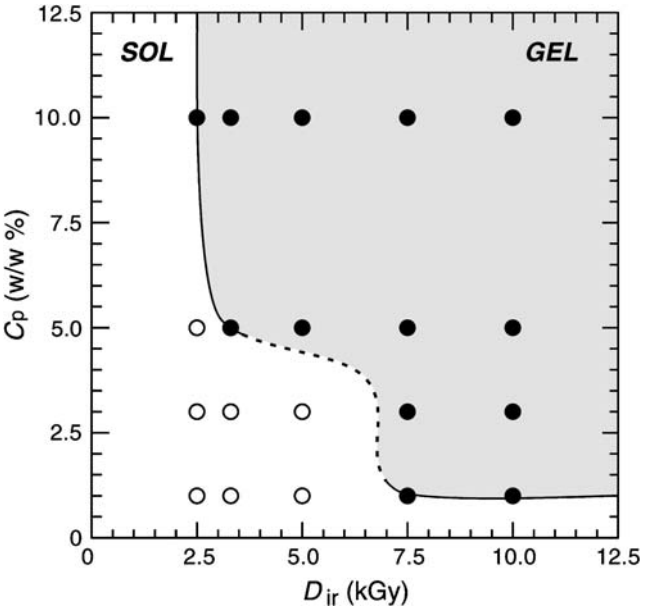


**Fig. 1** Sol–gel phase diagram of the PNiPAAm-water system after irradiation of γ-rays at ice bath temperature. The diagram was given as a function of polymer concentration ($C_p$) and irradiation dose ($D_{ir}$). *Solid lines linked by a broken line* show a relation between the critical polymer concentration ($C_{pc}$) and the gelation dose ($D_g$) with a prediction in the range indicated by the *broken line*

poly(vinyl alcohol) solutions [19, 20]. As a result, we found that RPIG and RPNG with different crosslink densities can be obtained by controlling either or both of $C_p$ and $D_{ir}$ so as to be higher than these thresholds (i.e., $C_{pc}$ and the $D_g$). In the later experiments, however, the gelation was made at a fixed $C_{pc}$ of 5% *w*/*w* and at a range of $D_{ir}$ from 5 to 30 kGy because the resulting gel was easy to handle even when taking it out of the glass capillary with the smallest internal diameter (i.e., 0.29 mm).

### Effect of temperature on the equilibrium swelling

Figures 2 and 3 show the swelling curves given by an equilibrium diameter ($d_{eq}$) for the radiation-crosslinked gels (RPIG and RPNG) obtained at $D_{ir}$=10, 20, and 30 kGy. Also shown in each figure for comparison are the results of the corresponding Bis-crosslinked gels (CIG and CNG) that were prepared at a fixed value of the molar concentration ratio ([*B*]/[*M*]) of Bis to monomer (NiPAAm or NnPAAm).

From the results of RPIG (Fig. 2), several important features are apparent: (1) An increase of $D_{ir}$ leads to a slight but significant decrease of the transition temperature ($T_c$) around which the change of $d_{eq}$ is very sharp but seems to become continuous, (2) the $T_c$ values of each RPIG are close to the LCST of PNiPAAm and higher by about 1 °C than that of CIG (as a typical example of Bis-crosslinked gels), (3) all the values of $d_{eq}$ at a swollen state ($<T_c$) decrease with increasing $D_{ir}$, but the $d_{eq}$ values of fully

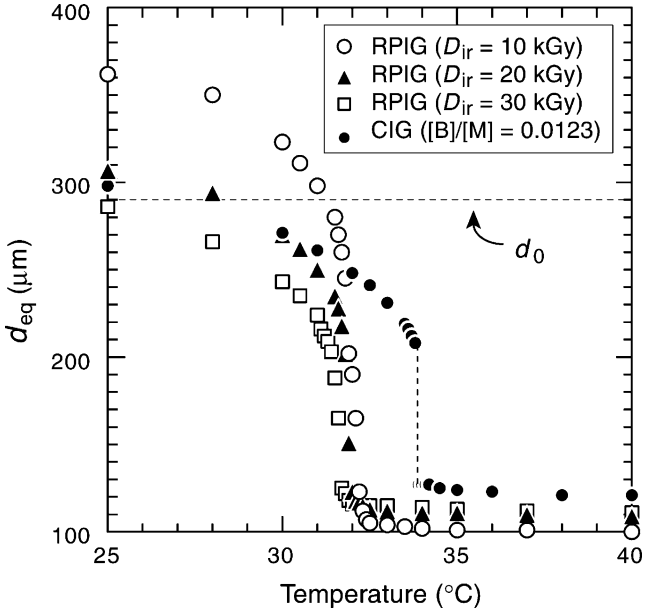


**Fig. 2** Temperature dependence of equilibrium diameter ($d_{eq}$) for radiation-crosslinked gels (RPIG) obtained from PNiPAAm at different irradiation doses ($D_{ir}$). Data for a chemically crosslinked gel (CNG) from NiPAAm was shown for comparison. $d_0$ (=290 μm) denotes the diameter in preparation

collapsed gels at temperatures $>T_c$ are close each other and hardly vary with $D_{ir}$, and (4) these $d_{eq}$ values are smaller than that of CIG.

The radiation-crosslinked RPNG (Fig. 3) exhibits similar trends to RPIG with respect to the effects of temperature and $D_{ir}$. However, each $T_c$ of RPNG is lower by about 10 °C than that of the corresponding RPIG. The other differences

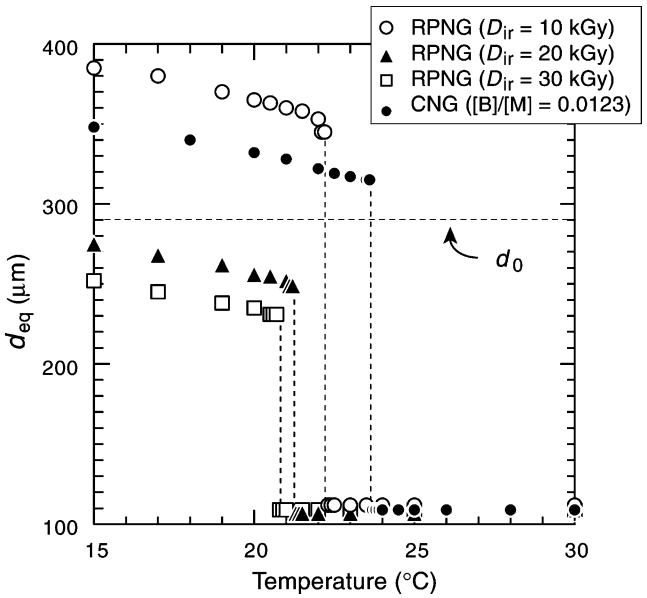


**Fig. 3** Temperature dependence of $d_{eq}$ for RPNG from PNnPAAm and for CNG from NnPAAm. For more details, see the caption of Fig. 2

between RPNG and RPIG as well as between RPNG and CNG are (a) The change of $d_{eq}$ at the $T_c$ for RPNG is obviously discontinuous in contrast to that for RPIG, (b) the $D_{ir}$-dependent decrease of $T_c$ is clearly seen in RPNG than in RPIG, and (c) under a fully collapsed sate, there is little difference in the $d_{eq}$ values between RPNG and CNG.

The NiPAAm and NnPAAm monomers have the same chemical composition but different stereochemical structures. The difference in LCST between PNiPAAm and PNnPAAm in water, as well as in $T_c$ between CIG and CNG, can be understood as a result of the primary (or monomer) structure-dependent difference of hydrophobic interaction, the magnitude of which is much stronger for NnPAAm than PNiPAAm. In other words, a liner side chain of NnPAAm is stiffer than a branched side chain of NiPAAm, thereby the hydrophobic hydration is predominant near the side chain of NnPAAm. Then, it is natural to consider that an increase of $D_{ir}$ leads to increasing the crosslink density, lowering the $T_c$ and also reducing the $d_{eq}$ at temperatures $<T_c$. The difference in the discontinuity at the transitions of RPIG and RPNG may be discussed in terms of their shrinking kinetics (see the next section).

Another important information from the temperature changes of $d_{eq}$ is that at 20 °C, the $d_{eq}$ of RPNG prepared at $D_{ir}\geq 20$ kGy is smaller than the $d_0$ value (see Fig. 3). We intend in this study to evaluate the structural inhomogeneity of gels from the DLS measurements at 20 °C using the samples prepared at ice bath temperature. Thus, the gel at 20 °C should be in a swollen state under which the $d_{eq}$ needs to be larger than the $d_0$ (see the "Experimental" section). Taking this into account, we employed the RPIG samples prepared at $D_{ir}<20$ kGy and the RPNG at $D_{ir}\leq$ 20 kGy in most of the later experiments.

## Swelling and shrinking kinetics

We used a set of the radiation-crosslinked gels (RPIG and RPNG) obtained at $D_{ir}=10$ kGy, as well as of the chemically crosslinked gels (CIG and CNG) at $[B]/[M]=0.0123$, all of which have a $d_0$ value of 1 mm. The cell temperature was rapidly changed, allowing the gel to swell or shrink, that is, from 30 °C (a swollen state) to 40 °C (a completely collapsed state) and vice versa for RPIG and CIG and from 18 °C (a swollen state) to 28 °C (a completely collapsed state) and vice versa for RPNG and CNG (see Figs. 2 and 3). Diameter ($d_t$) at time ($t$) for a gel was determined using its VTR image, then a normalized diameter ($d_n$) was obtained by

$$d_n = \frac{d_t - d_c}{d_s - d_c} \tag{4}$$

where $d_s$ and $d_c$ are equal to the $d_{eq}$ of a gel under a swollen and completely collapsed state at a given temperature,

respectively. For a gel spherical in shape and when its volume change is small, $\tau$ in Eq. 1 is theoretically related to its radius change ($\Delta a$) with $t$ by $\Delta a \sim \left(6\Delta a_0/\pi^2\right)$ $\exp(-t/\tau)$, where $\Delta a_0$ is the total radius change (see Eq. 10 in [5]). We used the gel cylindrical in shape, so that this relation may not be directly applied to our gels in the swelling and shrinking processes. However, it has been demonstrated that even for cylindrical gels, their swelling–shrinking kinetics can be studied by examining the time course of natural logarithm of $d_n$ (e.g., see [21] and [22]).

As can be seen from Fig. 4 (swelling process), the values of $\ln d_n$ increase linearly or very rapidly with time from 0 to 100 s, then gradually converges to zero. In all the cases, an equilibrium swelling was established within 30–60 min. In the swelling kinetics for all the types of gels, there seems to be no difference to be discussed. In contrast, in the shrinking kinetics (Fig. 5), there is a marked difference which is complicated depending on the kinds of source and on the crosslinking methods (recall Table 1). Thus, we concentrate on the shrinking process for each gel.

For a gel sphere (radius ~0.23 mm at 30 °C; $T_c$ ~38 °C), its shrinking process has been reported to be as [5] (1) The gel begins shrinking in which it keeps its spherical shape up to 70–90% of the initial radius; (2) after that the shrinking stops for a certain period of time, referring to as the "plateau period," and at the end of this period, bubbles appear on the surface of the gel; and (3) at the same time of the appearance of the bubbles, the gel resumes shrinking in which the bubbles initially swell, stop swelling, shrink, and finally disappear as the gel radius approaches to the final equilibrium size. To these three time domains, the different

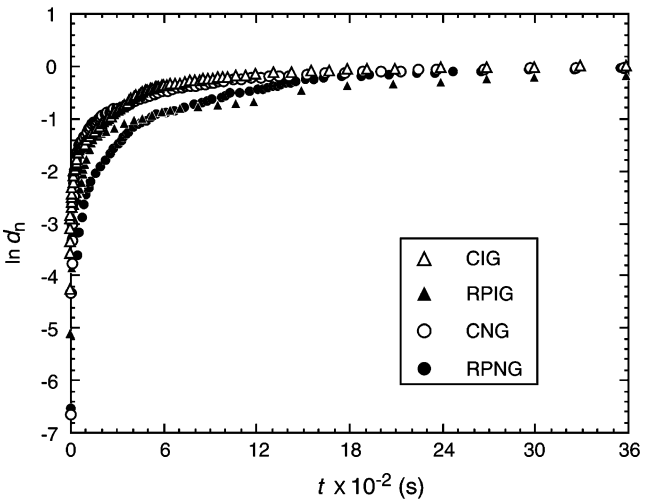


**Fig. 4** Changes of the natural logarithm of normalized diameter ($d_n$) with time ($t$) during the swelling of NiPAAm-based gels (CIG and RPIG) and NnPAAm-based gels (CNG and RPNG). The ambient temperature was rapidly lowered from 40 °C to 30 °C for CIG and RPIG, as well as from 28 °C to 18 °C for CNG and RPNG

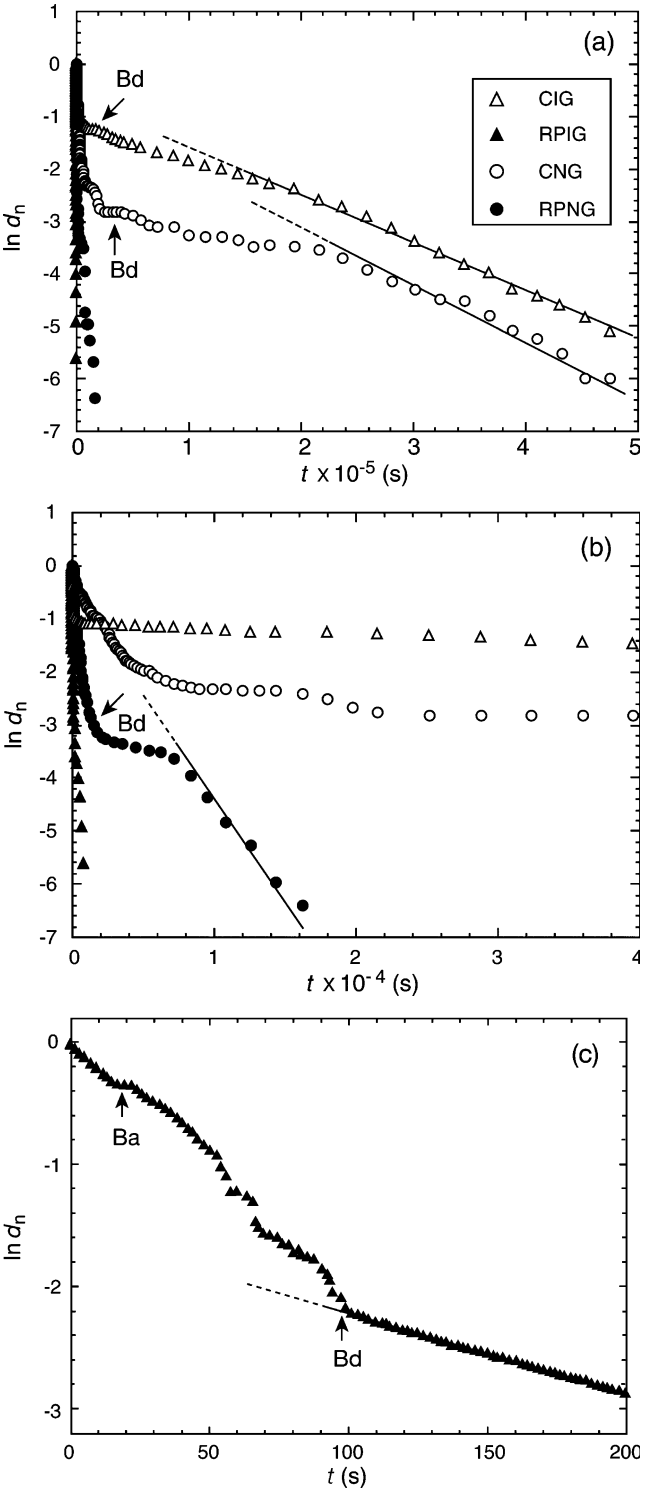


**Fig. 5** Changes of $\ln d_n$ with $t$ during the shrinking of NiPAAm-based gels (CIG and RPIG) and NnPAAm-based gels (CNG and RPNG). The ambient temperature was rapidly raised from 30 °C to 40 °C for CIG and RPIG, as well as from 18 °C to 28 °C for CNG and RPNG. The data from the early time points (0 to $4\times10^4$ s) in **a** are replotted on expanded time scales in **b** and **c**. The appearance of bubbles on the gel surface and their disappearance are indicated by Ba and Bd, respectively

$\tau$ values were then assigned: $\tau_1$ for shrinking period shown in (1), $\tau_p$ for plateau period in (2), and $\tau_2$ for shrinking period in (3). Note that in [5], the $\tau_2$ was determined under conditions where the gel has bubbles on its surface.

In our experiments, bubbles were observed in the shrinking (and also swelling) process for all of the gel samples. After the disappearance of the bubbles, the shrinking continued, the magnitude of which varied depending on the sort of gel. The plateau period before the appearance of the bubbles was only within 20 s for all the gels other than CIG, for which the bubbles appeared at 52 s and disappeared at 5.9 h. In contrast to spherical gels, a fine cylindrical gel having bubbles on its surface causes difficulties in determining the diameter with a high precision. Moreover, the plots after the disappearance of the bubbles cannot be fitted by only one straight line (compare each graph in Fig. 5). From these reasons, we did not estimate the values of $\tau_1$, $\tau_p$, and $\tau_2$. Nevertheless, it is very clear from Fig. 5 that the rate of overall shrinking is faster in the order of RPIG > RPNG > CNG > CIG.

During the plateau period, a thick and dense layer of collapsed polymer network, which is impermeable to the inner fluid, formed on the gel surface. It seems that this impermeable barrier temporarily prevents the gel from shrinking further. The appearance of the bubbles in the end of the plateau period is considered to resemble the local swelling of weak portions of an "inflated balloon," so that when the bubble is expanded or disappeared, the surface layer is no longer impermeable to the fluid and then the gel starts to shrink again. Taking these into account, we paid attention to the shrinking kinetics after the disappearance of the bubbles. This allows to fit the time course of natural logarithm of $d_n$ by a liner line and thereby to estimate $\tau$ accurately. The values of $\tau$ for each sample obtained from a linear line in Fig. 5 are shown in Table 2, together with the range between the maximum and minimum values of $d_n$ over which a good linear relationship was obtained at correlation coefficients larger than 0.99. It is found that the order of the rate of overall shrinking as mentioned above may be quantitatively given by the $\tau$ which is neither $\tau_1$ nor $\tau_2$. To make more clear that the $\tau$ is an indicator for characterizing the shrinking of gels, we studied the $d_0$ dependence of $\tau$ using RPIG which showed the fastest shrinking kinetics. As can be seen from Fig. 6, the results (circles and triangles) of the gels crosslinked at $D_{ir}$=10 and 20 kGy may be given by a liner line with a slope of 2, meaning that $\tau \propto l^2$ (see Eq. 1 in the "Introduction"). The gels crosslinked at $D_{ir}$=30 kGy provide a slope less than 2 (see square symbols), suggesting that an increase of $D_{ir}\geq$20 kGy would cause an "unusual" structure of gel networks in the case not only of PNiPAAm but also of PNnPAAm (recall that $d_{eq}<d_0$ even at 15 °C for RPNG prepared at $D_{ir}\geq$20 kGy).

Another important knowledge from Table 2 is the range in which the ln$d_n$ vs $t$ plot exhibits a linearity. The minimum $d_n$ values for all the gels are within 0.003 and 0.007, indicating close to a completely collapsed state. However, the maximum $d_n$ values are within 0.11 and 0.17 for the gel composed of NiPAAm monomer units (i.e., CIG and RPIG) and within 0.07 and 0.03 for the gel of NnPAAm monomer units (CNG and RPNG). These results mean that in the latter gel system, the most of volume collapse occurred before a linear decrease of ln$d_n$ (note that such collapsed gels contain 20–25% *w*/*w* of water). Thus, it seems that a strong hydrophobic interaction among the NnPAAm monomer units in both radiation-crosslinked and Bis-crosslinked gels causes a rapid formation of a thick and dense layer of collapsed polymer network on the gel surface. This well explain the difference in the magnitude of the discontinuity at the transition between RPIG and RPNG (see the previous section). Nevertheless, in either the NiPAAm- or NnPAAm-based system, the shrinking becomes faster in the radiation-crosslinked gels than in the Bis-crosslinked gels, to which we must pay attention when evaluating the microscopic inhomogeneity of gels.

**Table 2** Values of $\tau$ obtained from Fig. 5

| Gel[a] | $\tau$ (s) | Range of $d_n$ |
|---|---|---|
| CIG | $1.10\times10^5$ | 0.166–0.007 |
| CNG | $9.14\times10^4$ | 0.016–0.003 |
| RPIG | $1.47\times10^2$ | 0.110–0.002 |
| RPNG | $2.59\times10^3$ | 0.022–0.003 |

[a] See Table 1 for abbreviations

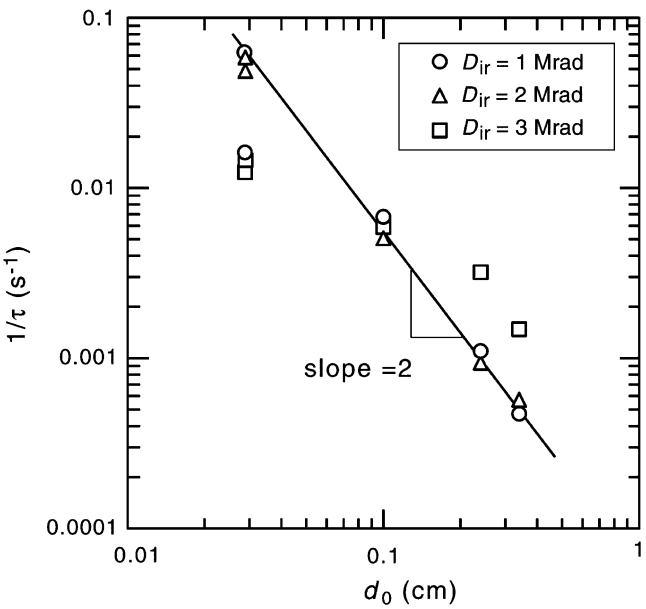


**Fig. 6** Logarithmic plots of $1/\tau$ vs $d_0$ as a function of $D_{ir}$ in the shrinking process of RPIG

On the crosslinking densities of RPIG and RPNG

It needs to know the crosslinking density for the radiation-crosslinked gels when their shrinking characteristics are compared with those of the Bis-crosslinked gels. We thus attempted to estimate the amount of crosslinks per the total of monomer units in a gel, the value of which should be equivalent to the $[B]/[M]$ as used in the Bis-crosslinked gels. In general, radiation yield ($G_x$) is defined as moles of produced or consumed chemicals per energy absorption of 100 eV [23]. In the case of radiation crosslinking of polymers, $G_x$ may be expressed as crosslinks per 100 eV. There are several methods for estimating $G_x$, among which we employed equilibrium swelling experiments. The concentration of effective chains ($V_e$ in mol/g) was then given as (see "Appendix"):

$$V_e = -\frac{\frac{v}{V'}\left\{\ln\left[1-\frac{C_p}{\rho_p}\left(\frac{V_0}{V}\right)\right]+\frac{C_p}{\rho_p}\left(\frac{V_0}{V}\right)+\chi\left(\frac{C_p}{\rho_p}\right)^2\left(\frac{V_0}{V}\right)^2\right\}}{\left(\frac{C_p}{\rho_p}\right)\left[\left(\frac{V_0}{V}\right)^{1/3}-\frac{1}{2}\left(\frac{V_0}{V}\right)\right]}. \tag{5}$$

Here, $V_0$ is the volume of gel in preparation, $V$ is the volume of gel after swelling (i.e., volume of a "fully" swollen gel at a given temperature), $V'$ is the molar volume of water (18 $cm^3$/mol), $v$ is the specific volume of polymer, $C_p$ (0.05 g/$cm^3$) is the concentration of polymer in pregel solution, $\rho_p$ is the density of polymer, and $\chi$ is the Flory interaction parameter (0.5 from [24]). If chain ends are ignored, $V_e$ is simply equal to $1/\overline{M}_c$, where $\overline{M}_c$ is the number-average molecular weight between two successive crosslinks. When the effect of chain ends is included, the $V_e$ becomes

$$V_e = \frac{1}{\overline{M}_c} - \frac{2}{\overline{M}_n} \tag{6}$$

where $\overline{M}_n$ is the number-average molecular weight of the initial polymer. If the sol fraction is small or negligible, $G_x$ (in crosslinks per 100 eV) is related to $D_{ir}$ (in kGy) by $G_x = 4.82\times10^6 \Big/ \left(\overline{M}_c D_{ir}\right)$. In our gel systems, the chain-end effects must be included, so that the following relation was used:

$$V_e = \frac{G_x D_{ir}}{4.82\times10^6} - \frac{2}{\overline{M}_n}. \tag{7}$$

When plotting $V_e$ against $D_{ir}$, we may thus obtain a straight line. The slope allows to calculate $G_x$, and the intercept is equal to $-2/\overline{M}_n$.

The polymers (PNiPAAm or PNnPAAm) in our pregel solution seem to be sufficiently crosslinked (see Fig. 1), indicating that the sol fraction may be negligible. Therefore, we may determine all the terms in Eq. 6 when $\rho_p$ (=1/$v$) is known. At the present stage, unfortunately, there are no studies reporting the $\rho_p$ value of PNiPAAm and/or PNnPAAm. In addition, it is not easy to determine these values with a sufficient accuracy. Then, we took notice of the fact that there is little difference in the $\rho_p$ values between poly(2-hydroxyethyl methacrylate) ($\rho_p$=1.274 g/$cm^3$; see [25]) and poly(vinyl alcohol) ($\rho_p$=1.269 g/$cm^3$; see [26]). This allows us to assume that an approximation of $\rho_p$~1.27 g/$cm^3$ is permissible for both polymers within experimental errors in determining $V_0/V$ as $(d_{eq}/d_0)^3$. Figure 7 shows the plots of $V_e$ vs $D_{ir}$ for RPIG and RPNG. A straight line was not obtained over the whole range of $D_{ir}$ because $d_{eq}<d_0$ at $D_{ir}<20$ kGy and at 25 °C for RPIG (see Fig. 2), as well as at $D_{ir}\leq20$ kGy and at 15 °C for RPNG (see Fig. 3). In the other ranges, however, there is a linear relationship between $V_e$ and $D_{ir}$ (correlation coefficients >0.95). As a result, we obtained the following $G_x$ values in crosslinks per 100 eV—7.50 for PNiPAAm and 9.67 for PNnPAAm. Using the these data, the ratio ($R_{C/M}$) of crosslinks to monomer units (both in molecules per gram) at different $D_{ir}$ levels was calculated from

$$R_{C/M} = 6.24\times10^{16}\frac{G_x D_{ir} M_0}{N_A f_{w,p}} \tag{8}$$

where $M_0$ denotes the molecular weight (113) of the NiPAAm or NnPAAm monomer, $N_A$ is Avogadro's number, and $f_{w,p}$ is the weight fraction (0.05) of the polymer of a pregel solution. Note that a temperature dependence of $R_{C/M}$

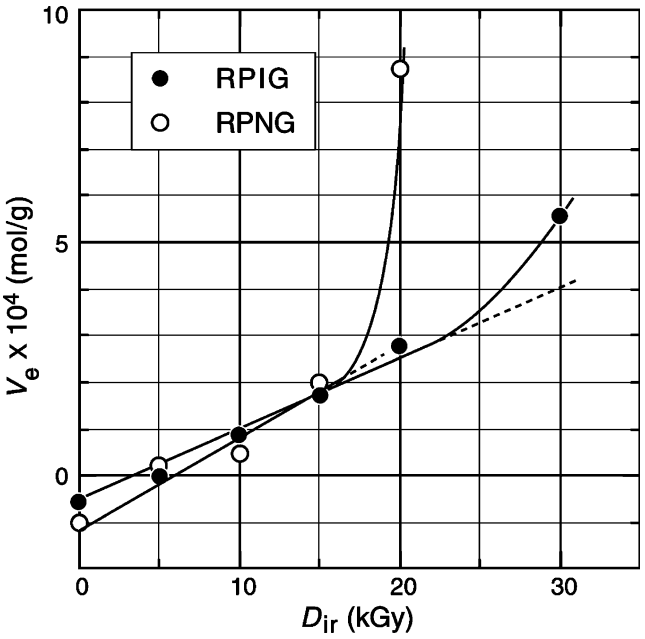


**Fig. 7** Dependence of effective chain concentration ($V_e$) on irradiation dose ($D_{ir}$). $V_e$ at a given $D_{ir}$ was determined from the average of three $d_0/d_{eq}$ data obtained using the gels with $d_0$=0.29, 1.0, and 2.4 mm at 25 °C for RPIG and at 15 °C for RPNG. The values at $D_{ir}$=0 were calculated from the $\overline{M}_n$ of both polymers (PNiPAAm and PNnPAAm) using a relation of $-2/\overline{M}_n$

would not be considered in the usual gels but must be in the thermosensitive gels because "physical crosslinks" could be formed from hydrophobic association among the polymer segments. Therefore, in the strict sense, the $R_{C/M}$ obtained here is the sum of covalently bonded monomer units and physically associated polymer segments (even if the latter effect is smaller than the former). This has been considered in the following discussions.

## DLS of gels

As described in the "Introduction", the presence of structural inhomogeneities of gels may be studied by the DLS experiments. Figure 8 shows the processes of DLS measurements and the data analyses using CIG as a typical example. When DLS was performed at a certain position of the gel, we may obtained an intensity–intensity time correlation function ($g^{(2)}(\tau)$). As shown in Fig. 8a, the data are well fitted with Eq. 2 in the "Introduction"; thus, we may obtain an apparent diffusion coefficient ($D_A$). Also obtained in this measurement is a time-averaged scattering intensity ($\langle I\rangle_T$). Repeating the DLS measurements at different positions of the same gel, we may collect many set of the $D_A$ and $\langle I\rangle_T$ data, from which both $\langle I_F\rangle_T$ and $D_L$ in Eq. 3 can be obtained. In practice, we used the following equation transformed from Eq. 3

$$\frac{\langle I\rangle_T}{D_A} = \frac{2}{D_L}\langle I\rangle_T - \frac{\langle I_F\rangle_T}{D_L} \tag{9}$$

and plotted $\langle I\rangle_T/D_A$ against $\langle I\rangle_T$. As can be seen from Fig. 8b, the plot shows a straight line of which the slope and intercept allow calculation of $\langle I_F\rangle_T$ and $D_L$. Another important analysis of DLS data is to examine a fluctuating speckle pattern using the $\langle I\rangle_T$ values at many measuring positions. Figure 8c shows the position dependence of $\langle I\rangle_T$, from which $\langle I\rangle_E$ can be obtained.

The DLS measurements were performed with the four kinds of gels shown in Table 1, which were prepared at different molar ratios of Bis to the monomer or at different irradiation doses. In Fig. 9, the results are summarized as a function of $[B]/[M]$ or $R_{C/M}$ (i.e., crosslinking density). There are few changes of $\langle I_F\rangle_T$ as an indicator of the dynamic concentration fluctuations arising from the thermal motion of network polymers (see Fig. 9b). In contrast, the $\langle I\rangle_E$ and $D_L$ vary depending on the crosslink density (see a and c in Fig. 9). These dependencies exhibit differences both in the constituent monomer of gels and in the crosslinking method; therefore, let us first look at changes

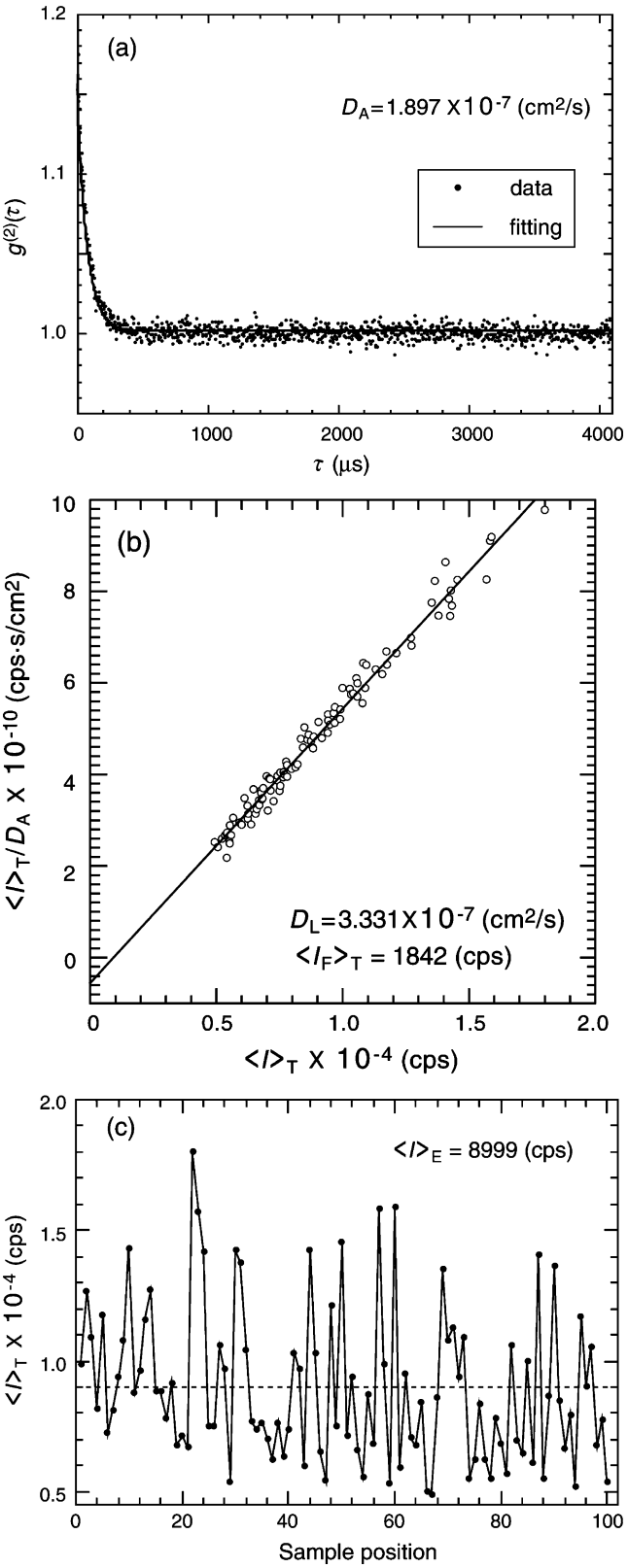


**Fig. 8** Typical example of analyses of DLS data for Bis-crosslinked NiPAAm gel (CIG) obtained at $[B]/[M]$=0.0123. **a** Intensity–intensity time correlation function ($g^{(2)}(\tau)$) for determining the apparent diffusion coefficient ($D_A$). **b** Plots of $\langle I\rangle_T/D_A$ vs $\langle I\rangle_T$ for determining both collective diffusion coefficient ($D_L$) and dynamic concentration fluctuations ($\langle I_F\rangle_T$). **c** Time averaged scattering intensity ($\langle I\rangle_T$) vs sample positions for determining the ensemble averaged scattering intensity ($\langle I\rangle_E$). Note that the measurements were performed at 100 positions of the gel (see the "Experimental" section)

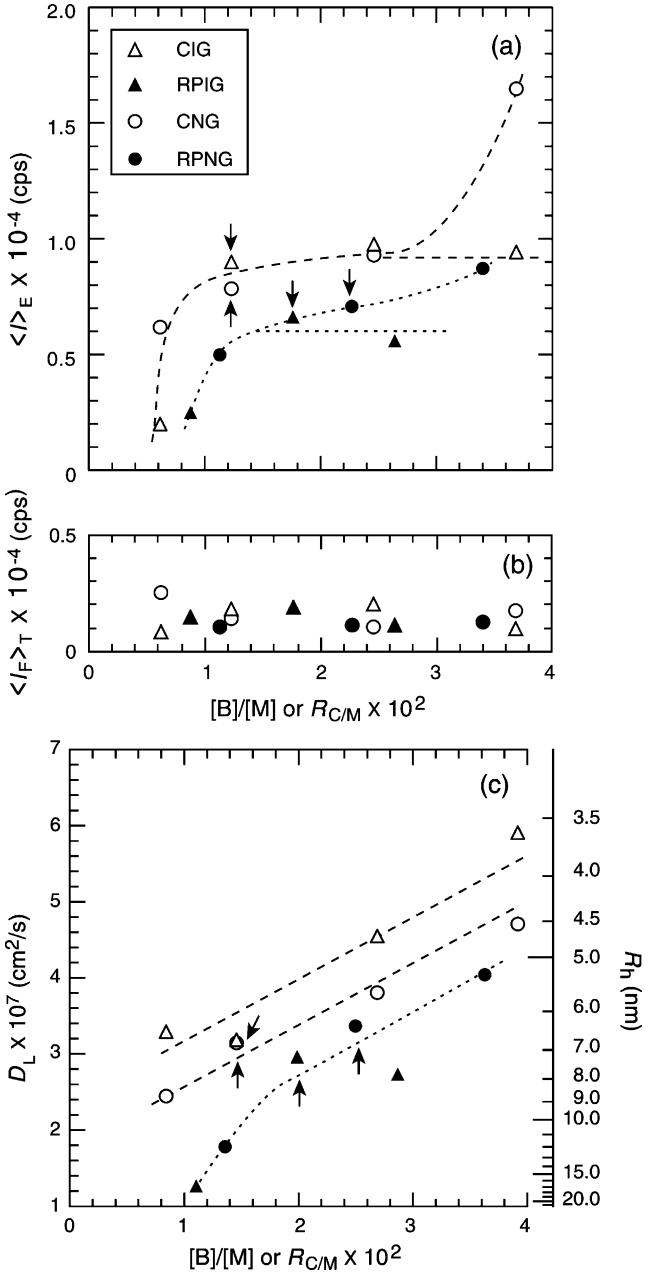


**Fig. 9** Results of DLS as a function of crosslinking density ([*B*]/[*M*] or $R_{C/M}$) for all of the gels in Table 1. **a** Ensemble averaged scattering intensity ($\langle I\rangle_E$), **b** dynamic component of the concentration fluctuations ($\langle I_F\rangle_T$), and **c** cooperative diffusion coefficient ($D_L$). Hydrodynamic radius ($\langle R\rangle_h$) that is equivalent to the corresponding $D_L$ is shown on the *right ordinate* of **c**. [*B*]/[*M*]=$6.15\times10^{-3}$~$3.69\times10^{-2}$ for CIG and CNG. $R_{C/M}$=$8.78\times10^{-3}$ ($D_{ir}$=5 kGy)~$2.64\times10^{-2}$ ($D_{ir}$=15 kGy) for RPIG and $1.13\times10^{-2}$ ($D_{ir}$=5 kGy)~$3.40\times10^{-2}$ ($D_{ir}$=15 kGy) for RPNG. *Dashed lines* on the figure serve to guide the eye only

of $\langle I\rangle_E$ that is the ensemble-averaged scattering intensity as the average of $\langle I\rangle_T$. The $\langle I\rangle_E$ is subjected to a change in the static inhomogeneities originating from (1) the dynamic critical fluctuations of the polymer solution at the onset of gelation and (2) the domain formation caused by the microphase separation during the gelation process, both of which are permanently frozen in the gel structure (see the "Introduction"). Taking these into consideration, we may say that the addition of a slight amount of crosslinks leads to a rapid increase in the static inhomogeneities; see near [*B*]/[*M*] or $R_{C/M}$ ~0.01. Upon further addition of crosslinks, the inhomogeneities frozen in CIG and RPIG level off at a certain value, but those in CNG and PRNG increase after passing through a plateau region. The radiation-crosslinked gels show the $\langle I\rangle_E$ values smaller than those of the chemically crosslinked gels over all the range studied, allowing to conclude that the level of the inhomogeneities is lower in the former than in the latter one.

At the onset of the chemical crosslinking, small polymer chains with "branches" could be formed as a precursor of polymer networks. This is quite different from the case in which long linear chains of polymers with a molar mass of several thousand (in our case) are crosslinked immediately with γ-rays (note that there are two types of crosslinking processes: intermolecular and intramolecular crosslinking [20]). Thus, in the radiation crosslinking, it is natural to consider either or both of (a) keeping at a low level of the static inhomogeneities and (b) a few effects of the crosslink density ($R_{C/M}$) on the static inhomogeneities. Indeed, this is the case in our experimental data. Also, the $\langle I\rangle_E$ of the gels used in the shrinking measurements is larger in the order of RPIG < RPNG < CNG < CIG (see plots indicated by arrows in the figure). This order agrees with that of $\tau$ in Table 2. As mentioned in the previous section, however, there are uncertainties in the determination of $R_{C/M}$. Therefore, the present data can only suggest but not conclude that the shrinking kinetics of gels is accountable for by the $\langle I\rangle_E$ from DLS.

From Fig. 9c, it is found that the $D_L$ values of the radiation-crosslinked gels are smaller than those of the chemically crosslinked gels. If $D\cong D_L$, the $\tau$ in Eq. 1 becomes larger, leading to the slow kinetics, contrary to the experimental results. The $D_L$ is the quantity depending on the dynamic fluctuation of a gel network. Therefore, we are able to handle it in the same way as estimating the hydrodynamic radius ($\langle R\rangle_h$) of polymers or colloids from DLS data using the Stokes–Einstein relationship of $D_L \approx kT/6\pi\eta\langle R\rangle_h$, where $k$ is the Boltzmann constant, $T$ is the absolute temperature, and $\eta$ is the solvent viscosity (0.010063 dyn·cm$^{-2}$·s at 20 °C). The right ordinate of Fig. 9c shows the $\langle R\rangle_h$ that is equivalent to the corresponding $D_L$. It seems that an increase in $D_L$ is due to a decrease in the fluctuation "size" of the network with increasing [*B*]/[*M*] or $R_{C/M}$. This becomes more clear in the case of the radiation-crosslinked gels because (1) the $\langle R\rangle_h$ of our polymers (PNiPAAm and PNnPAAm) before the addition of crosslinks is within the range of 15 to 19 nm, (2) these are close to the $\langle R\rangle_h$ values at a range of $R_{C/M}$ ~0.011 (i.e., a low addition of

crosslinks), but (3) a considerably smaller $\langle R\rangle_h$ can be estimated at the same [*B*]/[*M*] region. The $D_L$ ranging from $3\times10^{-7}$ to $6\times10^{-7}$ $cm^{-2}$·s is close to that of globular proteins such as human serum albumin and lysozyme, for which the corresponding $\langle R\rangle_h$ is from 4 to 7 nm (e.g., see [27]). Therefore, it seems that a microdomain with a size similar to that of a protein is formed in the chemically crosslinked gels. Such a domain could be composed of highly branched and inhomogeneously crosslinked polymer networks, like "nanogel" particles for which we have demonstrated the structural difference from "hard" colloids such as proteins and polymer latexes using DLS and SLS (e.g., see [28] and references therein). The existence of nanogel-like domains in CIG or CNG would lead to a large increase in the value of $\langle I\rangle_E$ as the measure of the built-in static inhomogeneities.

The results somewhat different from the present study have been reported in the swelling–shrinking kinetics as well as in the dependencies of $\langle I\rangle_E$ and $D_L$ upon the crosslink density for the NiPAAm-based gels crosslinked with Bis and γ-rays [13]. However, there is a big difference in the preparation methods of gels. For example, in [13], the aqueous solution of "raw" polymers was directly subjected to the γ-ray irradiation (see the "Introduction"). In addition, a wide range of $D_{ir}$ (20–50 kGy at 0 °C) was used for the radiation crosslinking of PNiPAAm. Recall, we suggested that for RPIG an increase of $D_{ir}\geq20$ kGy causes an "unusual" structure of the gel networks, at least in the comparison of their swelling–shrinking kinetics and microscopic structures (see Figs. 2, 5, and 7). From these reasons, it is difficult to discuss the differences between the results in [13] and in ours.

## Conclusions

We studied the swelling–shrinking kinetics using the NiPAAm and NnPAAm unit-based gels which were crosslinked either with Bis or γ-rays. A marked difference was observed in the temperature-induced shrinking processes of these gels. The rate of overall shrinking was faster in the order of RPIG (radiation-crosslinked PNiPAAm gel) > RPNG (radiation-crosslinked PNnPAAm gel) > CNG (chemically crosslinked NnPAAm gel) > CIG (chemically crosslinked PNiPAAm gel). Experimentally, this means that the shrinking rate is strongly influenced by whether the gel is prepared from the monomers with Bis or from the polymers with γ-rays. To make more clear this aspect at the microscopic level of gel networks, the DLS measurements were carried out as a function of the crosslink density. Then, we examined the crosslink density dependence of the ensemble-average scattered intensity and the diffusion coefficient, the values of which can be related to the static inhomogeneities frozen in the gel structure and to the dynamic fluctuation of polymer segments in the gel, respectively. We concluded that the results from DLS do not "completely" account for the differences observed in the shrinking kinetics for all the gels, due to accuracy in the determination of crosslink densities. However, it has become apparent that the ensemble-averaged scattering intensity and the diffusion coefficient for the chemically crosslinked gels were larger than those of the radiation-crosslinked gels. This suggest that the chemical crosslinking results in the formation of a small domain composed of highly branched and inhomogeneously crosslinked polymers due to the microphase separation during the gelation; therefore, allowing to conclude that the slow shrinking kinetics of the Bis-crosslinked gels is due to the highly nonuniform spatial distributions of polymer network concentration and crosslinking density. In other words, the fast kinetics observed in the shrinking processes of the radiation-crosslinked gels can be related to the homogeneous addition of crosslinks among the polymers to form the gel.

**Acknowledgment** The author (E.K.) would like to acknowledge the late Dr. Toyoichi Tanaka (Professor of Department of Physics and Center for Materials Science and Engineering, MIT, Cambridge) for his useful suggestions and comments in our studies of gels in early 1990s. This work was supported in part by Grants-in-Aid for Scientific Research to E.K. from the Ministry of Education of Japan (no. 08558092 and no. 09875232), the Japan Society for the Promotion Science (no. 15350127, no. 8655089, and no. 20550183), the New Energy and Industrial Technology Development Organization (NEDO), Japan, as well as from University of Tsukuba.

## Appendix

The volume of a relaxed gel, $V_{g,r}$, after crosslinking but before swelling, and the volume of a swollen gel, $V_{g,\,s}$, are given as

$$V_{g,r}=\frac{w_{a,r}-w_{h,r}}{\rho_h} \tag{10}$$

$$V_{g,s}=\frac{w_{a,s}-w_{h,s}}{\rho_h} \tag{11}$$

where $w_{a,r}$ denotes the weight of the relaxed gel in air, $w_{h,r}$ is the weight of the relaxed gel in such organic solvents as *n*-hexane, and $\rho_h$ is the density of an organic solvent (*n*-hexane in this case). Moreover, $w_{a,s}$ and $w_{h,s}$ represent the weight of the swollen gel in air and in *n*-hexane, respectively. Similarly, the volume ($V_p$) of dry polymer (used for gel preparation) may be given by

$$V_p=\frac{w_{a,d}}{\rho_p} \tag{12}$$

where $w_{a,d}$ is the weight of the polymer in air and $\rho_p$ is the density of the polymer. Note that in our case $w_{a,d}$ is

equivalent to the weight of polymers in preparation, but if there is a gel with an unknown amount of polymer constituents, the value of $w_{a,d}$ have to be determined with a "completely" dried gel.

Next, let us consider the polymer volume fraction ($v$) of gels. Denoting $v=v_r$ for the relaxed gel and $v=v_s$ for the swollen gel, we may write as

$$v_r = \frac{V_p}{V_{g,r}} \tag{13}$$

$$v_s = \frac{V_p}{V_{g,s}} \tag{14}$$

Thus, the equilibrium swelling equation can be expressed as follows:

$$\frac{1}{\overline{M}_c} = \frac{2}{\overline{M}_n} - \frac{\frac{v}{V'}\left[\ln(1-v_s) + v_s + \chi(v_s)^2\right]}{v_r\left[\left(\frac{v_s}{v_r}\right)^{1/3} - \frac{1}{2}\left(\frac{v_s}{v_r}\right)\right]} \tag{15}$$

Here, $\overline{M}_c$ is the number-average molecular weight between crosslinks, $\overline{M}_n$ is the number-average molecular weight of polymer chain before crosslinking, $\chi$ is the Flory interaction parameter, $v$ is specific volume of polymer, and $V'$ is molar volume of water.

Taking into account our experiments reported in the text, we can make the following approximations:

$$V_{g,r} = V_0 \tag{16}$$

$$V_{g,s} = V \tag{17}$$

$$V_p = \frac{w_{a,d}}{\rho_p} = \frac{V_0 C_p}{\rho_p} \tag{18}$$

where $V_0$ is the volume of the gel in preparation, $V$ is volume of gel in a swollen state at a given condition, and $C_p$ is the concentration of polymer in pregel solution. Consequently, we have the following relations:

$$v_r = \frac{V_p}{V_{g,r}} = \left(\frac{V_0 C_p}{\rho_p}\right)\left(\frac{1}{V_0}\right) = \frac{C_p}{\rho_p} \tag{19}$$

$$v_s = \frac{V_p}{V_{g,s}} = \left(\frac{V_0 C_p}{\rho_p}\right)\left(\frac{1}{V}\right) = \frac{C_p}{\rho_p}\left(\frac{V}{V_0}\right) \tag{20}$$

$$\frac{v_s}{v_r} = \frac{V_{g,s}}{V_{g,s}} = \frac{V_0}{V} \tag{21}$$

As a result, the concentration of effective chains, $V_e$ (in mol/g), can be written as:

$$V_e = \frac{1}{\overline{M}_c} - \frac{2}{\overline{M}_n} = -\frac{\frac{v}{V'}\left\{\ln\left[1-\frac{C_p}{\rho_p}\left(\frac{V_0}{V}\right)\right] + \frac{C_p}{\rho_p}\left(\frac{V_0}{V}\right) + \chi\left(\frac{C_p}{\rho_p}\right)^2\left(\frac{V_0}{V}\right)^2\right\}}{\left(\frac{C_p}{\rho_p}\right)\left[\left(\frac{V_0}{V}\right)^{1/3} - \frac{1}{2}\left(\frac{V_0}{V}\right)\right]} \tag{22}$$

## References


1. Tanaka T (1978) Phys Rev Lett 12:820
2. Tanaka T (1981) Sci Am 244:110
3. Tanaka T, Fillmore DJ (1979) J Chem Phys 70:1214
4. Tanaka T, Sato E, Hirokawa Y, Hirotsu S, Peetermans J (1985) Phys Rev Lett 55:2455
5. Sato-Matsuo E, Tanaka T (1988) J Chem Phys 89:1695
6. Kato T, Fujimoto K, Kawaguchi H (1994) Polym Gels Netw 2:307
7. Ogawa K, Wang B, Kokufuta E (2001) Langmuir 17:4704
8. Kabra BG, Gehrke SH (1991) Polym Commun 32:322
9. Wu XS, Hoffman AS (1992) J Polym Sci Part A 30:2121
10. Kokufuta E, Matsukawa S (1996) Ber Bunsenges Phys Chem 100:1073
11. Kishi R, Hirasa O, Ichijo H (1997) Polym Gels Netw 5:145
12. Kaneko Y, Sakai Y, Kikuchi A, Yoshida R, Sakurai Y, Okano T (1995) Macromolecules 28:7717
13. Norisuye T, Kida Y, Masui N, Tran-Cong-Miyata Q, Maekawa Y, Yoshida M, Shibayama M (2003) Macromolecules 36:6202
14. Sato-Matsuo E, Orkisz M, Sun ST, Li Y, Tanaka T (1994) Macromolecules 27:6791
15. Joosten JGH, McCarthy JL, Pusey PN (1991) Macromolecules 24:6690
16. Kokufuta E, Tanaka T, Ito S, Hirasa O, Fujishige S, Yamauchi A (1993) Phase Transit 44:217
17. Kokufuta E, Zhang Y-Q, Tanaka T, Mamada A (1993) Macromolecules 26:1053
18. Kokufuta E, Matsukawa S, Tanaka T (1995) Macromolecules 28:3474
19. Wang B, Mukataka S, Kodama M, Kokufuta E (1997) Langmuir 13:6108
20. Wang B, Kodama M, Mukataka S, Kokufuta E (1998) Polym Gels Netw 6:71
21. Ogawa K, Nakajima-Kambe T, Nakahara T, Kokufuta E (2002) Biomacromolecules 3:625
22. Ogawa Y, Ogawa K, Kokufuta E (2004) Langmuir 20:2546
23. Rosiak J, Olejniczak J, Charlesby A (1988) Radiat Phys Chem 32:691
24. Hirotsu S (1987) J Phys Soc Jpn 56:233
25. Peppas NA, Moynihan HJ, Lucht LM (1985) J Biomed Mater Res 19:397
26. Bray JC, Merrill EW (1973) J Appl Polym Sci 17:3779
27. Tsuboi A, Izumi T, Hirata M, Xia J, Dubin PL, Kokufuta E (1996) Langmuir 12:6295
28. Kokufuta E, Ogawa K, Doi R, Kikuchi R, Farinato RS (2007) J Phys Chem B 111:8634